Effect of long-term mechanical cycling and laser surface treatment on piezoresistive properties of SEBS-CNTs composites

Effect of long-term mechanical cycling and laser surface treatment on piezoresistive properties of SEBS-CNTs composites.

E. Padovano[a*], M.E. Bonelli[a], A. Veca[b], E. De Meo[b,c] and C. Badini[a]

[a] Politecnico di Torino, Department of Applied Science and Technology, Corso Duca degli Abruzzi 24, 10129, Torino, Italy
[b] C.R.F. S.C.p.A. – Group Materials Labs, C.so Settembrini 40, Torino, 10135, Italy
[c] University of Turin, Department of Chemistry and NIS Centre, Via P. Giuria 7, Torino, 10125, Italy
* Corresponding author: elisa.padovano@polito.it; +390110904708; fax: +390110904699

Abstract

The piezoresistive behaviour of SEBS-CNTs nanocomposites was investigated to evaluate their potential applications as strain sensors. Composites containing from 3%wt. to 7%wt. of CNTs were processed by injection moulding in order to evaluate the percolation threshold. The piezoresistive response under flexural strain of nanocomposites with a CNTs content above the percolation threshold was then studied. The nanocomposites showing the most promising performance were tested under cyclic conditions. Conductive tracks were then processed on nanocomposites surfaces (with 3 and 4% of CNTs) by means of a laser treatment. Samples with optimized laser tracks were then submitted to 1000 stretching/releasing cycles, showing improved piezoresistive performance.

Keywords: Polymer-matrix composites (PMCs); Electrical properties; Piezoresistive behaviour; Surface treatment

1. Introduction

Polymer based nanocomposites are recognized to provide the basis for the development of new technologies because of their noticeable properties. They can find applications in several fields as structural components or as functional materials for optical devices, electric flexible components, electromagnetic shields, biomedical devices and strain sensors. In fact, it is well known that the addition of nanofillers such as carbon nanotubes (CNTs) or graphene nanoplatelets (GNPs) to polymeric matrices improves the mechanical behaviour (strength, stiffness, creep and toughness) as well as the electric and thermal conductivity. These properties not only depend on the characteristics of the nanofiller and the polymeric matrix, but they are also greatly affected by the processing methods, the filler concentration, the homogeneity of filler dispersion and the orientation of fillers with high aspect ratio [1–6]. However, the extremely high conductivity of these nanofillers greatly enhances the conductivity of the insulating polymeric matrices when the filler concentration exceeds the percolation threshold, and a conductive network forms. The peculiar properties of these composites, whose electrical resistance changes with strain, can be exploited for sensors and actuators. When a conductive network is present inside the polymer matrix, an externally applied

stress can change the morphology of this network and cause a resistance increase or decrease depending on the kind of strain. A linear and significant change of resistance with strain, as well as the reproducibility of this phenomenon, is required for practical applications in sensors.

The effectiveness of CNTs for providing piezoresistive behaviour to polymers has been investigated during the last twenty years and deeply reviewed in some papers [7–10]. From the literature it seems that the influence of the polymer type on the piezoresistivity is small in comparison with the effect exerted by the kind of filler (for instance single-wall or multi-wall CNTs), its concentration and its distribution inside the matrix [7]. Piezoresistive effect is in fact due to the intrinsic piezoresistivity of CNTs, the tunnelling resistance of neighbouring CNTs and the modification of the conductive network formed by CNTs, due to the possible improvement or loss of contact among CNTs [7,8]. Also, the filler aspect ratio is considered to exert a strong influence on both the percolation threshold and the piezoresistivity [10–15].

The best piezoresistive response can be found when a proper filler concentration is adopted, while an increase or a decrease of concentration with respect to the ideal one is frequently detrimental [7,16,17]. In fact, when the filler concentration is very low the conductivity can be granted by tunnelling effect only, and the resistance is high. On the contrary, when a densely packed network forms because of rather high filler concentration, the modification of few conductive paths caused by strain has only minor influence on the electrical resistance of the composite. Therefore, the piezoresistive sensitivity of composites with high filler concentration can be poor. However, rather different values of the percolation threshold are reported in the literature for polymer-CNTs composites [7,9,18,19], even though percolation thresholds below 1% wt. were more frequently observed. Generally speaking, CNTs concentration just above the percolation threshold seems more suitable for achieving good strain sensitivity, since in this conditions a conductive network exists and the conductivity is not negligible [9,17,20]. On the other hand, good piezoresistive behaviour has been also observed for composites with rather high content of CNTs [10,16,18]. It was also found that the piezoresitive sensitivity increases with the concentration, while the response repeatability becomes poor and hysteresis appears far above the percolation threshold [21].

Most of the papers dealt with the piezoresistivity under tensile strain, but the behaviour under compressive or flexural strain was also investigated [7–9,22]. The monotonic change of resistance with the strain increase was observed for many composites, but only less frequently the resistance modification under cyclic strain variation was investigated [9], and only rarely the materials were submitted to a high number of cycles (namely 100 or 1000 cycles) [16,23]. The sensitivity of piezoresistivity to the extent of the strain or pressure and the kind of applied stress (tensile, compressive, flexural) and the possible phenomenon of saturation were also investigated [7,19,21].

Thin composite films [12,17–19,24–27], as well as thermoplastic and elastomeric matrices [10,17–19,21,27–30], seem a good choice for the production of flexible and wearable devices. On the other hand, bulk piezoresistive composites were processed by conventional techniques like melt mixing and additive manufacturing by fused deposition modelling [14,18,31]. Chemical [24], thermal [30] and laser [32] post processing treatments were also investigated with the aim of improving the piezoresistive properties of the polymer-CNTs composites.

In the present paper the piezoresistive behaviour of nanocomposites with styrene-b-(ethylene-co-butylene)-b-styrene (SEBS) matrix and multiwall carbon nanotube was investigated. The main purpose is to investigate the influence on the composites piezoresistive response when different strains are applied (by varying the maximum displacement and the rate of displacement); moreover, the reproducibility of the piezoresistive properties over a high number of loading/unloading cycles was assessed. The piezoresistive behaviour of the material was also checked after performing a surface laser treatment.

2. Experimental

2.1 Materials

The piezoresistive behaviour of nanocomposites with a matrix of styrene-b-(ethylene-co-butylene)-b-styrene (SEBS) thermoplastic elastomer reinforced by carbon nanotubes (CNTs) was investigated. The nanocomposites were produced by diluting a masterbatch containing 7% wt. of CNTs with the unfilled matrix. Pellets of a masterbatch were produced by Kraiburg TPE (Waldkraiburg, Germany) using commercial SEBS (TC7LEZ-920) and NC7000 carbon nanotubes (Nanocyl S.A., Sombreville, Belgium) with an average length of 1.5 µm and a diameter of 9.5 nm, according to the producer datasheet. In order to produce the nanocomposites with different filler concentrations (3, 4, 5, 6 and 7% wt. of CNTs), pellets of the masterbatch were mixed with pellets of unfilled SEBS and then extruded using a twin screen extruder (Haake Eurolab).

2.2 Characterization

Two kinds of samples were processed by injection moulding (Babyplast 6/10P): bars with size 80x10x4 mm^3 were produced for both resistance measurements and electro-mechanical tests, while plates 110x60x2 mm^3 in size were used for optimizing the laser writing process.

2.2.1 Electrical resistance

Two-wires surface resistance measurements were performed by using a multimeter (Keithley 2700E, resistance up to 120 MΩ). The surface resistance was measured on both moulded sample bars and conductive tracks obtained by laser scribing (sets of 3 samples). Square electrodes 10x10 mm^2 were created 40 mm apart one each other by depositing a silver-based conductive paints on the surface of the as-processed bars; conductive wires were then embedded into the electrodes and

connected to the multimeter. In order to measure the resistance of the laser tracks, they were firstly cleaned by using an air jet with the aim of remove the carbonaceous particles which were not well adherent to the tracks; then dot-shaped electrodes were obtained by depositing the silver-based paint at the edges of the tracks.

2.2.2 Electromechanical tests

Electromechanical tests, consisting of three-point bending coupled with resistance measurements, were performed. The experimental set up is shown in Figure 1; it was specifically designed for measuring the strain and the resistance variation at the same time. The three-point bending was carried out by using a dynamometer (Instron 5544 with a load cell of 2kN) equipped with a potentiometer for the measurement of sample displacement; Bluehill software was used for the acquisition of load, stress, displacement and strain. The resistance was measured by a multimeter (Keithley 2700E). The Instron data acquisition system and the multimeter were interfaced with a computer exploiting Labview software, which collected all the experimental data.

Formerly, the variation of resistance during a loading/unloading cycle was recorded under different experimental conditions. Eighteen tests were carried out on composites: two samples containing 5% wt. and 6% wt. of CNTs respectively were tested by varying the displacement and the holding time at the maximum displacement (9 different experimental conditions were tested for each composition) in order to investigate how their piezoresistive response can be influenced by different ways of applying the strain.

Long-term electromechanical tests were also performed by repeating the loading/unloading cycles up to 1000 times on the same sample. The piezoresistive behaviour during cycling of composite samples was then compared with that displayed by the composites showing a conductive track (processed by laser functionalization as described in 2.2.3 section). The cycling test was repeated two times for each kind of investigated material.

2.2.3 Laser functionalization

The laser functionalization was performed under nitrogen atmosphere by using a pulsed CO_2 laser with wavelength of 10.6 μm and a maximum power of 100W. The processing parameters such as power delivered, writing speed, defocus, laser frequency and number of writing repetitions on each track were controlled by Flycad software. For each set of laser treatment conditions four parallel tracks with a length of 4 cm and 1 cm apart from each other were written on a composite plate with size 110x60x2 mm^3; their resistance was then measured. Also, the inter-track resistance and the aesthetic characteristic of the samples after functionalization were considered in order to select the best processing parameters. The microstructure of the composites was investigated by examining

their fracture surface (obtained after a storage period in liquid nitrogen causing the sample embrittlement) by means of a FE-SEM (Zeiss Merlin). The morphology of the conductive tracks was investigated by using a confocal profilometer (Leica DCM81).

Figure 1

3. Experimental results and discussion

3.1 Preliminary assessment of resistance and piezoresistivity behaviour

The microstructure of the nanocomposites with different amount of CNTs can be observed on their cryofracture surfaces (Figure 2). The carbon nanotubes are homogeneously dispersed inside the polymeric matrix and tend to align in the direction of the injection moulding, thus placing perpendicular to the fracture surface. No evidences of carbon nanotube agglomeration were found on the fracture surface of the masterbatch or on the fracture surface of the samples obtained by diluting it with unfilled SEBS.

Figure 2

The surface resistance of the composites with different amount of CNTs as reinforcement is compared in Table 1; the nanocomposites are labelled with the acronym of the matrix (SEBS) followed by the percentage of nanotubes. The resistance decreases as function of the increase of CNTs content, but not in a linear manner: this is due both to the formation of a conductive network and to the so called "skin effect". In fact, the percolation curves are "S-shaped" and the resistance suddenly decreases when the nominal content of CNTs increases just over the percolation threshold, because a continuous network of conductive filler forms. Moreover, it is well known [33–35] that the injection moulding causes the alignment of the carbon nanotubes along the injection direction. This alignment in the flow direction mainly occurs near the mould surface, where it leads to the reduction of tube-tube contacts and an impairment of network formation. In addition, it has been reported that during the moulding process the carbon fillers tend to migrate from the surface toward the sample core [36]. Therefore, the electrical resistance of the skin is higher than that of the sample core and the resistance measured on the surface is influenced by this skin effect. The percolation threshold for the surface electrical conductivity of the SEBS-CNTs composite under investigation can be placed at around 3-4% wt. of CNTs. In the composite with a CNTs content corresponding to the percolation threshold (3% of CNTs) the standard deviation (it was calculated for resistance values measured between two points on the sample surface) was very high. Owing to the rather low CNTs content the conductive network is inhomogeneous, and this results in different resistivity values measured in different directions and parts of the sample.

When a load is applied to a polymer/CNTs nanocomposite bar, an elastic strain formerly occurs. At the microscopic level, the polymeric chains are stretched and then they are forced to assume a linear shape. The CNTs that are placed in between the polymer chains are dragged from the change of

orientation and elongation of the chains, so they tend to align to the strengthening direction. For this reason, the number of entanglements and of points of contact between the CNTs decreases when elastic strain occurs; then the electrical resistance increases. When the elastic strain is removed, the chains tend to assume the pristine configuration and then the conductive network of CNTs is restored, with a consequent resistance decrease. This change of electrical resistance during loading and unloading is responsible for the piezoresistive behaviour of CNTs-based nanocomposites. This phenomenon can be, in principle, exploited for the fabrication of pressure sensors. However, several other requirements are needed for this application: the resistance variation should occur under small strain levels and contemporary to the deformation; in addition, the resistance variation should happen cyclically every time that a load is applied or relieved.

With the aim of assessing the suitability of the elastomeric nanocomposites under investigation for sensor applications, the effect of the mechanical strain on the piezoresistive behaviour was investigated under different loading conditions. Firstly, the piezoresistivity effect was studied during a single cycle of deformation and then the behaviour of nanocomposites during mechanical cycling was evaluated.

The first test involved the progressive bending (up to 10 mm of displacement) of the composite bars at the constant displacement rate of 10mm/min and the measurement of resulting resistance variation. The latter, reported as percentage of change with respect to the initial resistance value, is plotted in Figure 3 as a function of the time and the displacement.

Figure 3

For all the specimens the resistance increased when the displacement increased, but the curves showed different trends and slopes depending on the filler concentration. Samples with 3% or 4% of CNTs show high resistance values that change in an irregular manner with the displacement, and then they display bad piezoresistive behaviour. Samples with 7% CNTs shows resistance values that increase according to a not linear trend as function of the displacement increase. Actually, the resistance increases less than that expected under high displacements. When the CNTs concentration is high, not all the nanotubes change their orientation when the displacement increases; the nanotubes are in fact strongly interconnected within a network with several contact points that are hardly unleashed. Also according to Villmow et al. [35] the re-arrangement of CNTs caused by external stresses becomes more difficult with their concentration increases. Sample with 6% and overall sample containing 5% of nanotubes show an almost linear increase of resistance with the displacement; in particular SEBS-5 sample shows the maximum resistance percent variation (1.2%).

Conclusively, contents of CNTs just above the percolation threshold seem to grant the best piezoresistive response. SEBS-5 and SEBS-6 nanocomposites were therefore submitted to further tests which simulate the possible operating conditions experienced by a pressure sensor. Actually, a piezoresistive switch could be strained in different manners in operating conditions. Therefore, the samples were tested according to a cycle of loading and unloading, keeping constant the displacement rate (10mm/min), but changing the maximum displacement and the period of holding at the maximum displacement. Maximum displacements of 2, 5 and 10 mm and times of staying at the maximum displacement for 2, 5 and 10 seconds were adopted, thus performing nine tests for each sample composition, as shown in Table 2.

Figure 4 shows the displacement change occurring during one of these cycles (blue curve), the resistance variation expected for a material showing an ideal piezoresistivity behaviour (red dotted curve), and an example of real variation of electrical resistance (red curve).

Figure 4

Elastomers should display an elastic behaviour, and then they should recover the original size and shape when the load is removed. The movement of polymeric chains should also cause the recovery of the original configuration of the CNTs network, and the restoration of the pristine electrical resistance as well. However, relaxation phenomena can occur with some delay with respect to the load change. As a result, the curve depicting the real change of resistance with the displacement differs from the ideal one, as shown by the comparison between the two red curves in Figure 4. Although an ideal piezoresistive material should react to a displacement variation by changing immediately its resistance, some delay in the response and a signal instability were observed for the materials under investigation.

Moreover, the speed of resistance variation was found to be different from the speed of displacement variation in every part of the cycle; some resistance variation could be also detected when the displacement remained constant (maximum displacement and null displacement at the end of the cycle). The rate of resistance variation can be compared with the rate of displacement variation during loading and unloading in order to assess how much the piezoelectric behaviour deviates from the ideal one. Relaxation effects under a constant load should be also considered to this purpose.

The following parameters were then recorded to investigate the material behaviour under a single cycle: the speed of resistance increase during the displacement increase (v_1), the speed of resistance variation during the stay at the maximum displacement (v_2) and the speed of resistance decrease during the displacement decrease (v_3). The best piezoresistive behaviour can be observed when v_1 and v_3 are as close as possible to the displacement variation rate and when v_2 is close to zero.

The effectiveness of a piezoresistive device is also related to the extent of resistance variation when displacement changes, while resistance variation should not occur when the displacement is constant or null. In order to investigate the deviation from the ideal behaviour some parameters related to the resistance changes were also considered (Figure 4): maximum resistance variation during the loading step (ΔR_1), resistance decay during the stay at the maximum displacement (ΔR_2) and resistance deviation with respect to the initial one at the end of each cycle (R_b). Finally, an ideal piezoresistive behaviour should entail that the initial resistance is fully recovered as soon as the displacement is completely removed; therefore, the possible delay time (t) and the deviation from the initial resistance value at the end of the cycle (R_b) should be as little as possible. The values assumed by these parameters were calculated from each experimental curve. All the results are reported in Table 2.

A further parameter that could be considered is the v_3/v_2 ratio, that should be as high as possible, because it is related to the promptness to react to the start of unloading with a clear signal.

As an example, some experimental curves showing the resistance variation during cycles carried out under different conditions are reported in Figure 5.

It is evident that the resistance variation profile is affected by the cycling conditions. The results summarized in Table 2 show as the maximum displacement and the period of maintenance at the maximum displacement exert a great effect on the effectiveness of the piezoresistive material, as discussed in the following sections. Moreover, some differences can be seen for composites with different CNTs content.

3.1.1 Composite with 5%wt. of CNTs

An increase of the maximum displacement or of the holding time at the maximum load causes the increase of the resistance change (ΔR_1) and of the promptness of piezoresistivity response (v_1); the increase of maximum displacement also increases the resistance change speed when the load is progressively removed (v_3).

Figure 5

On the contrary, these parameters seem not to affect in a clear manner the time (t) required to recover the initial resistance value when the load is completely removed. As a matter of fact, not only there is always a delay in the recovery of the initial resistance after unloading, but the material continues to change its resistance in the minutes after unloading, giving rise to final resistance values that are different from the initial one (R_b). Actually, not negligible R_b values were found; it means that during a first cycle of loading and unloading some adjustment in the network of CNTs always occurred. During the stay at the maximum displacement the resistance slightly decreases and the speed of this variation (v_2) increases as function of the maximum displacement suffered by the

sample and of the holding time. Finally, the v_3/v_2 ratio clearly increases with the maximum displacement.

An increase of the holding time at the maximum displacement (and load) also causes the increase of both resistance variation and resistance speed of changing (ΔR_1 and v_1) during loading. However, this parameter does not affect in a clear manner the v_3/v_2 ratio, as it influences both v_3 and v_2 in the same manner. The recovery of the initial value of resistance requires increasing time (t) with the prolongation of the holding time at the maximum load. No clear correlations were found between the holding time and R_b.

Conclusively, the best piezoresistivity behaviour during the one-cycle test was observed when high values of maximum displacement and holding time were adopted.

3.1.2 Composite with 6%wt. of CNTs

In the case of composite containing 6%wt. of CNTs an increase of the maximum displacement causes the increase of both the resistance change and the resistance change speed during loading (ΔR_1 and v_1); a similar effect, but much less marked, was observed for v_3 during unloading. Unfortunately, also the resistance variation occurring meanwhile holding the load (ΔR_2, always very little) and its change speed (v_2) increase with displacement, which results in the decrease of the v_3/v_2 ratio. The time required to recover the initial resistance (t) increases with the displacement and the final resistance always differs from the initial one (even though a correlation between R_b and displacement was not found).

An increase of the holding time at the maximum displacement does not result in any improvement of piezoresistive response during the loading step (ΔR_1 and v_1), while a little beneficial effect was observed on the resistance variation rate during the displacement release (v_3). This parameter seems to have only a negligible effect on the resistance variation and resistance variation speed during holding (ΔR_2 and v_2); moreover, no correlation was found between this parameter and R_b. Anyway, ΔR_2 was always found very little. The prolongation of the holding time has also a detrimental effect on the index v_3/v_2. As already occurred for the composite containing 5% of CNTs, not negligible R_b values were found.

Conclusively, the piezoresistive behaviour of the nanocomposite containing 6% of CNTs is only slightly affected by the testing parameters. This is not surprising because the piezoresistive response is usually affected by the CNTs content, and high CNTs concentrations make the system less sensitive to strain.

When the CNTs concentration increases, the resistance decreases, as more percolation paths are present inside the conductive network. When this happens the change of conductivity caused by the application of a load becomes less important as the number of conductive paths is high under both

loading and unloading conditions. For this reason, the conditions of load application (defined as maximum strain achieved, period during which the load is hold and then time available for network re-arrangement) affect less the piezoresistive response of the composite with 6% of CNTs. Anyway, in this case good piezoresistive response was also observed when the loading/unloading cycle was carried out with rather small displacement and short holding time.

3.2 Piezoresistivity observed under cycling conditions

A pressure sensor, based on piezoresistive effect, should operate for long periods and also properly react to stress and displacement variations several times. In order to investigate the suitability of the nanocomposites under investigation for exploitation in pressure sensor devices they were submitted to high number of cycles. The samples with 5% wt. and 6% wt. of CNTs were submitted to 100 cycles of strain variations in the following conditions: displacement increase/decrease rate of 10 mm/min, maximum displacement of 10 mm (for SEBS 5%CNTs) or 2 mm (for SEBS 6%CNTs), no holding period at the maximum displacement. On the base of the results previously obtained, a high displacement value (which enhances the resistance change) was adopted for testing SEBS with 5% wt. of CNTs, while a lower displacement was sufficient to obtain suitable resistance variation when testing SEBS with 6% wt. of CNTs. The electrical signal given by the sample with 5% of CNT showed instability since the first cycling period; this is clearly depicted for the first ten cycles in Figure 6.

Figure 6

In the case of nanocomposite with 5% CNTs it is also clear that stress and strain are out of phase and a noisy electrical signal is obtained; some permanent deformation of the sample was also observed.

In the case of sample with 6% of CNTs a certain lack of coherence between electrical signal and displacement was observed, even though the specimens provided a signal during all the testing period (100 cycles). The resistance progressively decreased with the number of cycles increase, but the resistance variation during each cycle was kept almost constant (Figure 6B). The lack of coherence between the imposed displacement and the resistance variation can be explained on the base of the microstructure of the co-polymer SEBS. In these polymeric materials small blocks of styrene are alternated with longer ethylene-butylene blocks. These latter show lower elastic modulus and then greater elastic deformation, but the total deformation is hindered by the stiff styrene blocks. The soft blocks suffer more deformation during each cycle, here the chains stretch and tend to align and the strength of the bonds between the chains increases. On the other hand, the stiff styrene portion of the polymer hinders elastic deformation. The deformation is slowly, and then not completely recovered during the second part of the cycle, which results in some hysteresis.

During cycling the sample stiffness progressively increased, as shown by the fact that the load required to achieve the pre-fixed displacement progressively increased too. The CNTs were dragged by the movements of the polymeric chains, changed their relative position and the conductive network characteristics, thus causing a change of the overall resistance of the material. Conclusively the piezoresistive behaviour of these nanocomposites showed some lacks in terms of readiness to react to stress and capability of maintaining the electrical properties during long duration cycling. These drawbacks very likely would hinder the exploitation of these materials in pressure sensors. However, it is well known that the piezoresistivity of nanocomposites can be improved by using laser treatments.

3.3 Functionalization by laser treatment: writing of conductive tracks

The effect of the irradiation by a laser beam of the surface of a polymer/CNTs composite has been investigated in previous papers [32,37]. The laser beam causes the thermal decomposition of the polymeric matrix, and then the increase of CNTs concentration and material conductivity. This kind of functionalization can be exploited for the creation "in situ" of conductive tracks and it constitutes an attractive method for the realization of metal-free electrical circuits. The effectiveness of this surface laser treatment for improving the piezoresistive behaviour was also proved in previous investigations, for instance for PC-ABS/CNTs composites [32]. For this reason, in the present investigation this kind of treatment was also used to modify the piezoresistive response of the SEBS/CNT composites. The result of the laser treatment can vary depending on the parameters adopted for the laser writing. In fact, the laser power, the writing speed, the number of repetitions, the frequency and the focusing can greatly affect the final electrical resistance of the conductive tracks. Generally speaking, the amount of delivered energy, and then the severity of the thermal decomposition process, increases with the increase of the power and number of repetitions and decreases with the increase of the laser scan speed. Unfortunately, a too much severe laser treatment can result in a damage of the sample and then should be avoided for practical applications. The experimental conditions that allow to obtain the best conductivity improvement without any sample damage depend on the kind of nanocomposite and, in particular, on the kind of polymeric matrix. Therefore, the best experimental conditions for such a kind of functionalization should be assessed for each polymer/CNTs system.

Formerly, the laser writing parameters were optimized for the SEBS nanocomposites, and then the piezoelectric behaviour was tested on sample laser treated under these selected conditions. Since the laser treatment causes a conductivity increase, the composites containing 3% or 4% of CNTs were submitted to laser writing. Moreover, as showed in section 3.1, composites with rather high nanotubes content and low resistance do not show the best piezoresistive behaviour. On the

contrary, the composites with 3-4% of CNTs show a conductivity just below the percolation threshold, and their conductivity is expected to appreciably increase owing to the laser treatment. In order to assess the most suitable parameters for the laser writing process, several laser treatments were carried out and then the electrical properties of the resulting tracks were compared. The track resistance as well as the inter-track resistance were measured. The inter-track resistance must be very high in order to avoid short circuits. The morphology of the samples was also checked after the treatment; in fact, any change of shape or hole formation should be avoided.

On the base of previous experience in laser functionalization, the frequency was fixed at 30 kHz and the defocusing at 0 for all tests. Laser speeds of 100, 200 and 300 mm/s were coupled with powers values equal to 5, 10 and 20% of the total power available. These conditions were combined with 10, 20 and 30 laser runs for the composite with 3% of CNTs and with 5, 10 and 15 repetitions for the composite with 4% of CNTs. Fifty-four laser treated samples were obtained and for each of them the track resistance (measured on the four tracks), the inter-track resistance and the final integrity were investigated. The set of laser writing parameters are summarized in Table 3 with the relevant values of track and inter-track resistances (R_t and R_i respectively). The standard deviation calculated for each set of four tracks obtained under the same conditions shows that very poor reproducibility of resistance values can be achieved when low power and high writing speed are adopted. In these cases, the energy delivered by the laser is low and the treatment affects only the sample surface, where the network of CNTs is not very effective because of the previously mentioned skin effect. In several cases very high resistance, sometimes exceeding the measurement range of the multimeter (reported as OR), was measured between adjacent traces, while in other cases the inter-track conductivity was not negligible and therefore the set of adopted laser parameters inappropriate. Several experimental conditions caused visible damage of the specimens: trials 5-9, 14-18, 23-27 for composites with 3% CNTs and trials 1, 5, 6, 8, 9, 15, 18, 21, 24 for composites with 4% CNTs. Actually, too high energy delivered by the laser, due to high power and number of repetitions combined with low laser speed, has detrimental effect. Samples with poor track conductivity, too low inter-track resistance or showing some damage were discarded.

Only few of these sets of laser writing conditions seem suitable for processing properly conductive tracks on SEBS composites. The performances of the tracks showing acceptable characteristics are compared in Figure 7A for the samples with 3% of CNTs and in Figure 7B for the samples with 4% of CNTs. Also, the ratio between inter-track and track resistance is here reported.

Figure 7

Finally, the conditions used for trial T2 (P =5%, v=200 mm/s, N= 30 repetitions) and trial T12 (P =5%, v=100 mm/s, N= 10 repetitions) were selected respectively for the nanocomposite with 3%

and 4% of CNTs, and adopted for the further investigation on their piezoresistive behaviour. Using these processing parameters, a single track was obtained on SEBS-3 and SEBS- 4 samples bars, which were then submitted to cyclic electro-mechanical testing.

3.4 Piezoresistive behaviour of nanocomposites after laser treatment

The morphology of the laser tracks can be appreciated by using the confocal microscope (Figure 8). The comparison of Figures 8B and 8D highlights the major importance of the writing speed with respect to the number of repetitions. In fact, the two tracks show similar width but very different depth (d_z parameter in the track profiles). The track depth is around double in the sample with 4% of CNTs treated with a writing speed of 100 mm/s (half of the speed used for the sample with 3% of CNTs), even though only ten laser runs were performed.

Figure 8

These samples were submitted to bend strain cyclically (1000 cycles using a displacement rate of 10 mm/min and a maximum displacement of 2 mm), meanwhile their surface electrical resistance was measured. A displacement rate of 10 mm/min and a maximum displacement of 2 mm were adopted for testing, since these conditions proved to be suitable for composites with rather high CNTs concentration (see section 3.2) and the laser treatment causes the local enhancement of filler content. The resistance variation during cyclic tests versus the displacement is shown in Figure 9.

Figure 9

In both cases it can be seen that there is some instability during the initial cycles; in fact, the average resistance increases and the extent of resistance range changes. However, after a first period the system stabilizes. The enlargement of a portion of these curves allows to appreciate how the resistance changes in a coherent and prompt manner with the displacement (Figures 9B and 9D). In fact, the maximum and the minimum resistance values were always observed at the maximum and minimum displacement for both the nanocomposites. The resistance of the material before testing was never recovered at the end of each cycle because of the visco-elastic behaviour of these nanocomposites, which causes a delay in the restoration of the microstructure when the mechanical load is removed. Moreover, some differences in the behaviour of these two materials can be appreciated. The range of resistance variation was much wider, and the curve of resistance change was sharper for the composite containing 3% of CNTs, which gave the best result. Anyway, the laser functionalization was able to greatly improve the piezoresistive response of these nanocomposites. In fact, after the laser treatment the readiness of reacting to a mechanical stress and the reproducibility of the piezoresistive response during long term mechanical cycling appreciably increased. Conclusively, the laser treatment was able to generate tracks with a peculiar microstructure that behave in a different manner from composites with a high content of filler, well dispersed inside the matrix. In fact, the increase of the CNTs concentration in the SEBS matrix gave

no advantage for the piezoresistive response, while the laser action greatly improved it. Probably the laser treatment not only locally increases the filler concentration, but also gives rise to a very effective network constituted by CNTs and carbonaceous particles coming from the matrix pyrolysis.

However, some instability of the average resistance was still observed after the laser treatment, particularly during the initial cycling period. On the other hand, electronics can well offer the way of correcting this lack, so that the peculiar characteristics of this kind of nanocomposites can be exploited for fabrication of pressure sensors.

4. Conclusions

In the present study nanocomposites with SEBS matrix filled with CNTs were processed starting from a masterbatch by compounding with unfilled SEBS and injection moulding, thus obtaining a fairly good distribution of the nanotubes within the matrix. The threshold for the formation of a conductive network was observed at around 3% wt. of CNTs.

The composites with 5% wt. and 6% wt. of CNTs showed the best piezoresistive response. A higher CNTs concentration was detrimental for the piezoresistive behaviour because the conductive network is closely packed and its modification due to strain gives rise to small resistance variations only. The electrical resistance of these nanocomposites increased in an almost linear manner with the displacement increase because of the stretching of the macromolecular chain which caused the modification of the CNTs network. When the strain was released, the resistance decreased because of the restoration of the conductive network, which occurred with some delay with respect to the strain change. During the initial stretching/releasing cycles some adjustment of the conductive network and of the average material resistance happened. The experimental results showed that the resistance variation occurring during a single cycle depended on the strain variation profile. In fact, the maximum displacement, the displacement rate and the holding time of maximum displacement affected the piezoresistive response. During the maintenance of the maximum displacement some relaxation always occurred, resulting in a slight resistance decrease. The best piezoresistive response was observed for the composite with 5% of CNTs under high displacement and strain holding time. The effect of strain conditions became less important when the concentration of CNTs increased (e.g. 6% wt. of CNTs).

The repetition of the stretching/releasing cycle (100 cycles) put in evidence some lacks in the piezoresistive response of these nanocomposites. Initially the average resistance decreased, but the range of resistance variation only slightly changed during 100 cycles. The main lacks dealt with the readiness of reacting to strain variation and the mismatch between displacement and resistance

changes. These drawbacks hinder the exploitation of these materials for practical applications as piezoresistive switches.

Therefore, a laser surface treatment, causing the formation of conductive tracks, was exploited to improve the piezoresistive response. Since this treatment causes the local increase of CNTs concentration it was applied to composites with a filler content close to the percolation threshold. However, different combinations of laser processing parameters were required for different CNTs concentrations, in order to obtain tracks with enhanced conductivity and avoiding contemporary any macroscopic damage of the material.

Samples carrying conductive tracks processed under optimized conditions showed improved piezoresistive behaviour with respect to not functionalized SEBS/CNTs composites. The laser surface treatment allowed to achieve good reproducibility of the piezoresistive response and coherence between strain cyclically imposed and material resistance during 1000 stretching/releasing cycles.

Acknowledgement

This research did not receive any specific grant from funding agencies in the public, commercial, or not-for-profit sectors.

Experimental Data file “Dataset "Piezoresistive properties of SEBS-CNTs composites"”, is available on Mendeley Data, doi: 10.17632/pc4z4vkpfg.2

References

[1] D.G. Papageorgiou, Z. Li, M. Liu, I.A. Kinloch, R.J. Young, Mechanisms of mechanical reinforcement by graphene and carbon nanotubes in polymer nanocomposites, Nanoscale. 12 (2020) 2228–2267. https://doi.org/10.1039/c9nr06952f.

[2] Y. Li, X. Huang, L. Zeng, R. Li, H. Tian, X. Fu, Y. Wang, W.H. Zhong, A review of the electrical and mechanical properties of carbon nanofiller-reinforced polymer composites, J. Mater. Sci. 54 (2019) 1036–1076. https://doi.org/10.1007/s10853-018-3006-9.

[3] S. Wu, S. Peng, C.H. Wang, Multifunctional polymer nanocomposites reinforced by aligned carbon nanomaterials, Polymers (Basel). 10 (2018). https://doi.org/10.3390/polym10050542.

[4] K. Hosseinpour, A.R. Ghasemi, Agglomeration and aspect ratio effects on the long-term creep of carbon nanotubes/fiber/polymer composite cylindrical shells, J. Sandw. Struct. Mater. (2019). https://doi.org/10.1177/1099636219857200.

[5] A.R. Ghasemi, M. Mohandes, R. Dimitri, F. Tornabene, Agglomeration effects on the vibrations of CNTs/fiber/polymer/metal hybrid laminates cylindrical shell, Compos. Part B Eng. 167 (2019) 700–716. https://doi.org/10.1016/j.compositesb.2019.03.028.

[6] Y. Xiao, X. Zhang, W. Cao, K. Wang, H. Tan, Q. Zhang, R. Du, Q. Fu, Dispersion and Mechanical Properties of Polypropylene/ Multiwall Carbon Nanotubes Composites Obtained via Dynamic Packing Injection Molding, J. Appl. Polym. Sci. 104 (2007) 1880–1886. https://doi.org/DOI 10.1002/app.25852.

[7] N.H. Alamusi, H. Fukunaga, S. Atobe, Y. Liu, J. Li, Piezoresistive Strain Sensors Made from Carbon Nanotubes, (2011) 10691–10723. https://doi.org/10.3390/s111110691.

[8] W. Obitayo, T. Liu, A Review : Carbon Nanotube-Based Piezoresistive Strain Sensors, 2012 (2012). https://doi.org/10.1155/2012/652438.

[9] T. Yan, Z. Wang, Z. Pan, Flexible strain sensors fabricated using carbon-based nanomaterials : A review, Curr. Opin. Solid State Mater. Sci. 22 (2018) 213–228. https://doi.org/10.1016/j.cossms.2018.11.001.

[10] F. Aviles, A.I. Oliva-Avilles, M. Cen-puc, Piezoresistivity , Strain , and Damage Self-Sensing of Polymer Composites Filled with Carbon Nanostructures, 1701159 (2018) 1–23. https://doi.org/10.1002/adem.201701159.

[11] U. Szeluga, B. Kumanek, B. Trzebicka, Synergy in hybrid polymer / nanocarbon composites . A review, Compos. PART A. 73 (2015) 204–231. https://doi.org/10.1016/j.compositesa.2015.02.021.

[12] F. Avilés, A. May-pat, M.A. López-manchado, R. Verdejo, A. Bachmatiuk, A comparative study on the mechanical , electrical and piezoresistive properties of polymer composites

using carbon nanostructures of di ff erent topology, Eur. Polym. J. 99 (2018) 394–402. https://doi.org/10.1016/j.eurpolymj.2017.12.038.

[13] J. Cai, Y. Chen, J. Li, Y. Tan, J. Liu, X. Tang, X. Chen, M. Wang, Asymmetric deformation in poly (ethylene-co-1-octene)/ multi-walled carbon nanotube composites with glass micro-beads for highly piezoresistive sensitivity, Chem. Eng. J. 370 (2019) 176–184. https://doi.org/10.1016/j.cej.2019.03.223.

[14] K. Ke, V.S. Bonab, D. Yuan, I. Manas-zloczower, Piezoresistive thermoplastic polyurethane nanocomposites with carbon nanostructures, Carbon N. Y. 139 (2018) 52–58. https://doi.org/10.1016/j.carbon.2018.06.037.

[15] V. Eswaraiah, S.S. Jyothirmayee Aravind, K. Balasubramaniam, S. Ramaprabhu, Graphene-functionalized carbon nanotubes for conducting polymer nanocomposites and their improved strain sensing properties, Macromol. Chem. Phys. 214 (2013) 2439–2444. https://doi.org/10.1002/macp.201300242.

[16] X. Fu, Stretchable strain sensor facilely fabricated based on multi-wall carbon nanotube composites with excellent performance, J. Mater. Sci. 54 (2019) 2170–2180. https://doi.org/10.1007/s10853-018-2954-4.

[17] P. Zhang, S. Lei, W. Fu, J. Niu, G. Liu, J. Qian, J. Sun, The effects of agglomerate on the piezoresistivity of conductive carbon nanotube / polyvinylidene fluoride composites, Sensors Actuators A. Phys. 281 (2018) 176–184. https://doi.org/10.1016/j.sna.2018.08.037.

[18] Z. Sang, K. Ke, I. Manas-zloczower, Effect of carbon nanotube morphology on properties in thermoplastic elastomer composites for strain sensors, Compos. Part A. 121 (2019) 207–212. https://doi.org/10.1016/j.compositesa.2019.03.007.

[19] J. Vicente, P. Costa, J.M. Abete, A. Iturrospe, Electromechanical Properties of PVDF-Based Polymers Reinforced with Nanocarbonaceous Fillers for Pressure Sensing Applications, (n.d.).

[20] X. Yang, L. Sun, C. Zhang, B. Huang, Y. Chu, Modulating the sensing behaviors of poly (styrene-ethylene-butylene- styrene)/ carbon nanotubes with low-dimensional fi llers for large deformation sensors, Compos. Part B. 160 (2019) 605–614. https://doi.org/10.1016/j.compositesb.2018.12.119.

[21] S. Xu, H. Hu, L. Ji, P. Wang, Piezoresistive Properties of Multi-Walled Carbon Nanotube / Silicone Rubber Composites under Cyclic Loads with AC Excitation Piezoresistive Properties of Multi-Walled Carbon Nanotube / Silicone Rubber Composites under Cyclic Loads with AC Excitation, (2019). https://doi.org/10.1088/1742-6596/1168/2/022075.

[22] G. Spinelli, P. Lamberti, V. Tucci, L. Vertuccio, L. Guadagno, Experimental and theoretical

study on piezoresistive properties of a structural resin reinforced with carbon nanotubes for strain sensing and damage monitoring, Compos. Part B. 145 (2018) 90–99. https://doi.org/10.1016/j.compositesb.2018.03.025.

[23] S. Kumar, T.K. Gupta, K.M. Varadarajan, Strong , stretchable and ultrasensitive MWCNT / TPU nanocomposites for piezoresistive strain sensing, Compos. Part B. 177 (2019) 107285. https://doi.org/10.1016/j.compositesb.2019.107285.

[24] Y. Wang, S. Wang, M. Li, Y. Gu, Z. Zhang, Piezoresistive response of carbon nanotube composite film under laterally compressive strain, Sensors Actuators A. Phys. 273 (2018) 140–146. https://doi.org/10.1016/j.sna.2018.02.032.

[25] Q. Li, S. Luo, Q. Wang, Piezoresistive thin film pressure sensor based on carbon nanotube-polyimide nanocomposites, Sensors Actuators A. Phys. 295 (2019) 336–342. https://doi.org/10.1016/j.sna.2019.06.017.

[26] M. Li, J. Wang, S. Wang, Effect of microstructure on the piezoresistive behavior of carbon nanotube composite film Effect of microstructure on the piezoresistive behavior of carbon nanotube composite fi lm, (2019).

[27] S.M. Doshi, E.T. Thostenson, Thin and Flexible Carbon Nanotube-Based Pressure Sensors with Ultrawide Sensing Range, ACS Sensors. 3 (2018) 1276–1282. https://doi.org/10.1021/acssensors.8b00378.

[28] Y. Tan, J. Li, Y. Chen, X. Tang, J. Cai, J. Liu, M. Wang, Gentle crosslinking to enhance interfacial interaction in thermoplastic polyurethane / poly (ethylene-co-1-octene)/ multi-walled carbon nanotube composites for conductive improvement and piezoresistive stability, Polym. Test. 75 (2019) 142–150. https://doi.org/10.1016/j.polymertesting.2019.02.004.

[29] E. Subramani, S. Raman, K. Werner, S. Wießner, G. Heinrich, A. Das, High-performance elastomeric strain sensors based on nanostructured carbon fi llers for potential tire applications, Mater. Today Commun. 14 (2018) 240–248. https://doi.org/10.1016/j.mtcomm.2018.01.013.

[30] J. Ramon Dios, C. García-Astrain, P. Costa, S. Viana, Júlio César Lanceros-Méndez, Carbonaceous Filler Type and Content Dependence of, Materials (Basel). 12 (2019) 1405–1420.

[31] M. Kim, J. Jung, S. Jung, Y.H. Moon, Piezoresistive Behaviour of Additively Manufactured Multi-Walled Carbon Nanotube/Thermoplastic, (n.d.).

[32] A. Caradonna, C. Badini, E. Padovano, A. Veca, E. De Meo, M. Pietroluongo, Laser Treatments for Improving Electrical Conductivity and Piezoresistive Behavior of Polymer – Carbon Nanofiller Composites, (2019). https://doi.org/10.3390/mi10010063.

[33] J. Tiusanen, D. Vlasveld, J. Vuorinen, Review on the effects of injection moulding parameters on the electrical resistivity of carbon nanotube filled polymer parts, Compos. Sci. Technol. 72 (2012) 1741–1752. https://doi.org/10.1016/j.compscitech.2012.07.009.

[34] T.B. Nguyen Thi, S. Ata, T. Morimoto, T. Okazaki, T. Yamada, K. Hata, Visualizing electrical network in microinjection-molded CNT polycarbonate composite, Carbon N. Y. 153 (2019) 136–147. https://doi.org/10.1016/j.carbon.2019.07.019.

[35] T. Villmow, S. Pegel, P. Pötschke, U. Wagenknecht, Influence of injection molding parameters on the electrical resistivity of polycarbonate filled with multi-walled carbon nanotubes, Compos. Sci. Technol. 68 (2008) 777–789. https://doi.org/10.1016/j.compscitech.2007.08.031.

[36] C.M. Hong, J. Kim, S.C. Jana, Shear-induced migration of conductive fillers in injection molding, Polym. Eng. Sci. 44 (2004) 2101–2109. https://doi.org/10.1002/pen.20215.

[37] G. Colucci, C. Beltrame, M. Giorcelli, A. Veca, C. Badini, A novel approach to obtain conductive tracks on PP/MWCNT nanocomposites by laser printing, RSC Adv. 6 (2016) 28522–28531. https://doi.org/10.1039/c6ra02726a.

Figure Captions

Figure 1. Experimental set up for electromechanical testing.

Figure 2. Cryofracture surface of SEBS/CNTs nanocomposites: (A) 3% wt. of nanotubes, (B) 7% wt. of nanotubes.

Figure 3. Resistance change with the displacement increase.

Figure 4. Cyclic testing of nanocomposites: programmed displacement cycle (blue curve), ideal resistance variation (red dotted curve), and an example of experimental result of resistance change (red continuous curve). Speed of resistance variation (v1, v2, v3) and resistance changes ($\Delta R1$, $\Delta R2$) observed in the different parts of the cycle. Delay time for the recovery of the initial resistance (t) and deviation from the pristine resistance value at the end of the cycle (Rb).

Figure 5. Displacement and resistance variation during a cycle under different conditions for SEBS with 5% CNTs: displacement rate = 10 mm/min, (A) maximum displacement (MD) of 5 mm and stay at the maximum displacement = 2s; (B) MD of 5 mm and stay at the MD = 10s; (C) MD of 10 mm and stay at the MD = 2s; (D) MD of 10 mm and stay at the MD = 10s.

Figure 6. Piezoresistive response during repeated cycles: (A) SEBS-5 during the initial ten cycles, (B) SEBS-6 during 100 cycles.

Figure 7. Performance of conductive tracks obtained by laser writing on composite with (A) 3% of CNTs and (B) 4% of CNTs

Figure 8. Nanocomposite with 3% of CNTs after laser treatment (v= 200 mm/s, P= 5%, N= 30): profile of the track (B) measured along the red line (A); nanocomposite with 4% of CNTs after laser treatment (v= 100 mm/s, P= 5%, N= 10): profile of the track (D) measured along the red line (C).

Figure 9. Change of resistance (red curve) and displacement (blue curve) during mechanical cycling. (A) 1000 cycles performed on SEBS-3 (B) coherence of displacement and resistance variations during cycling of SEBS-3, (C) 1000 cycles performed on nanocomposite SEBS-4, (D) coherence of displacement and resistance variations during cycling of nanocomposite SEBS-4.

Figures

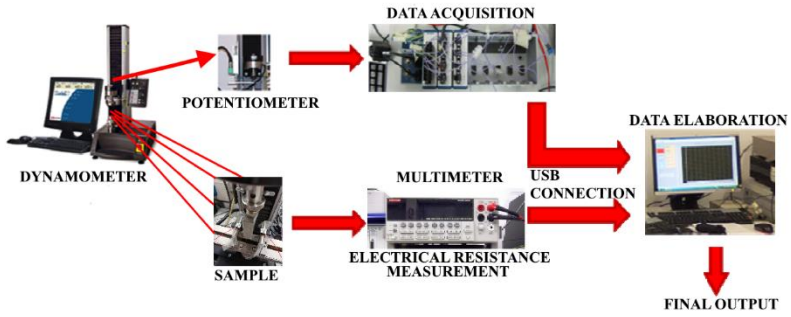

Figure 1

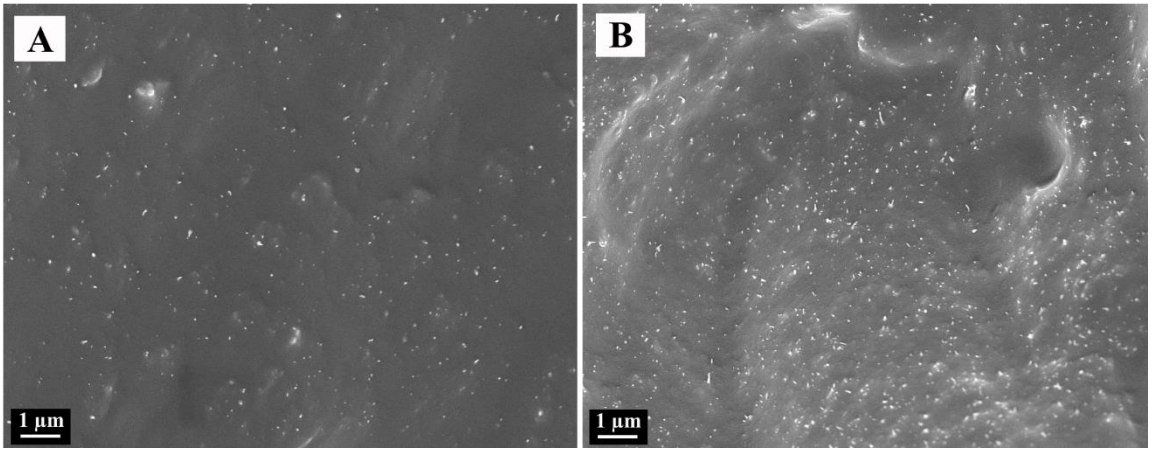

Figure 2

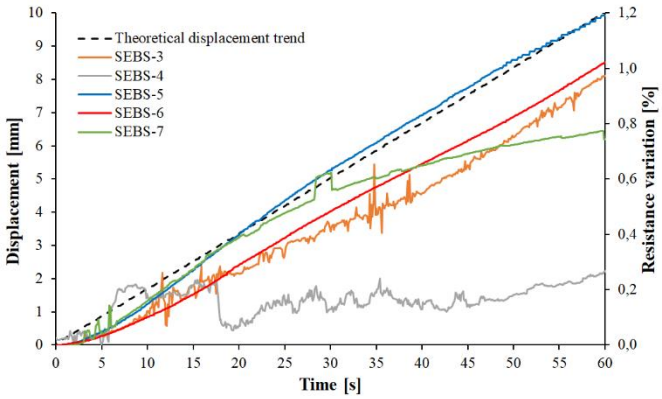

Figure 3

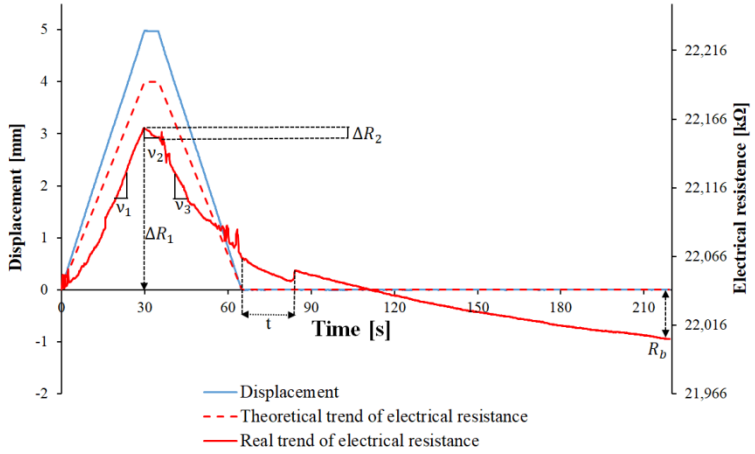

663

664 Figure 4

665

666

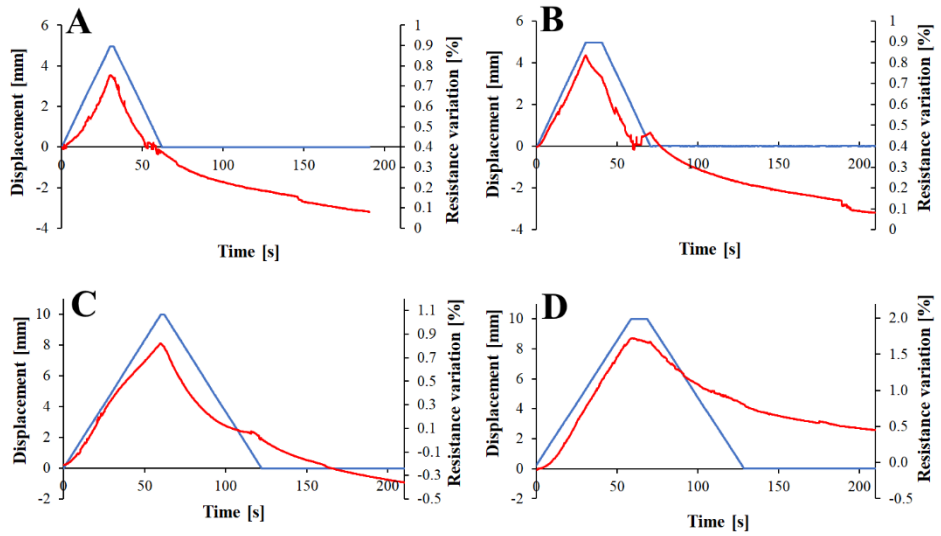

667

668 Figure 5

669

670

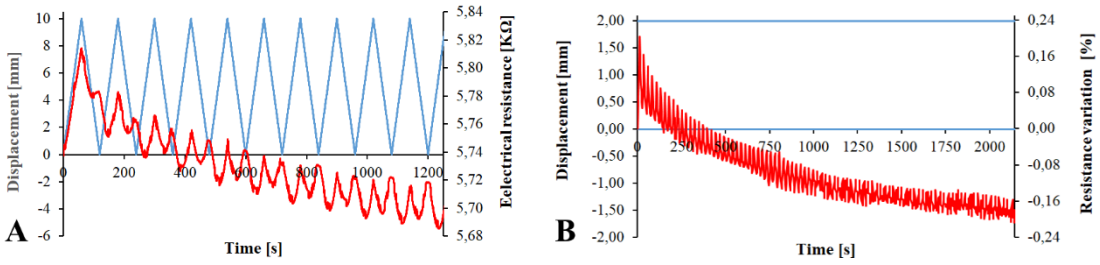

671

672 Figure 6

673

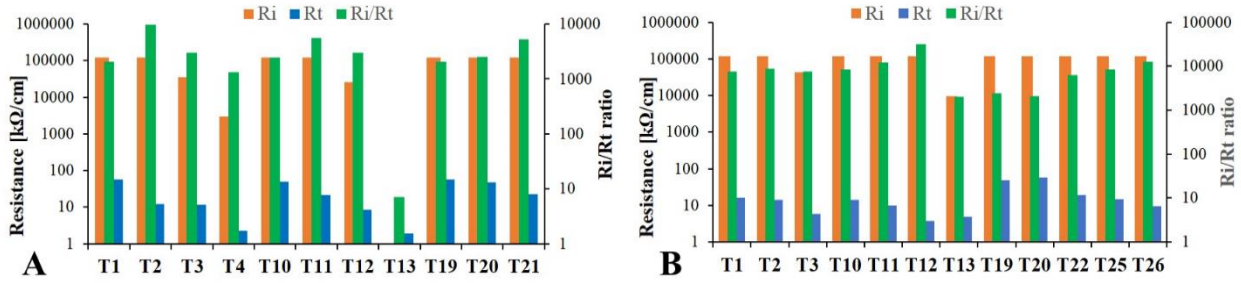

Figure 7

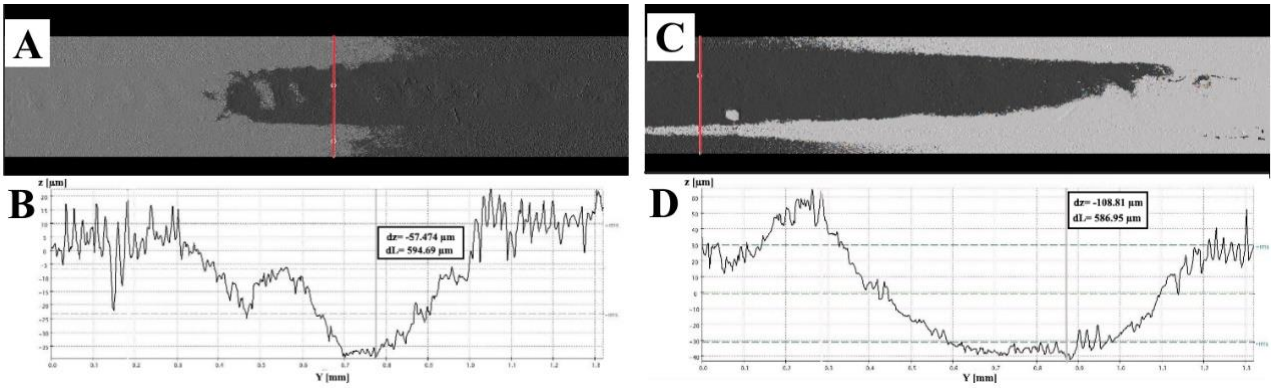

Figure 8

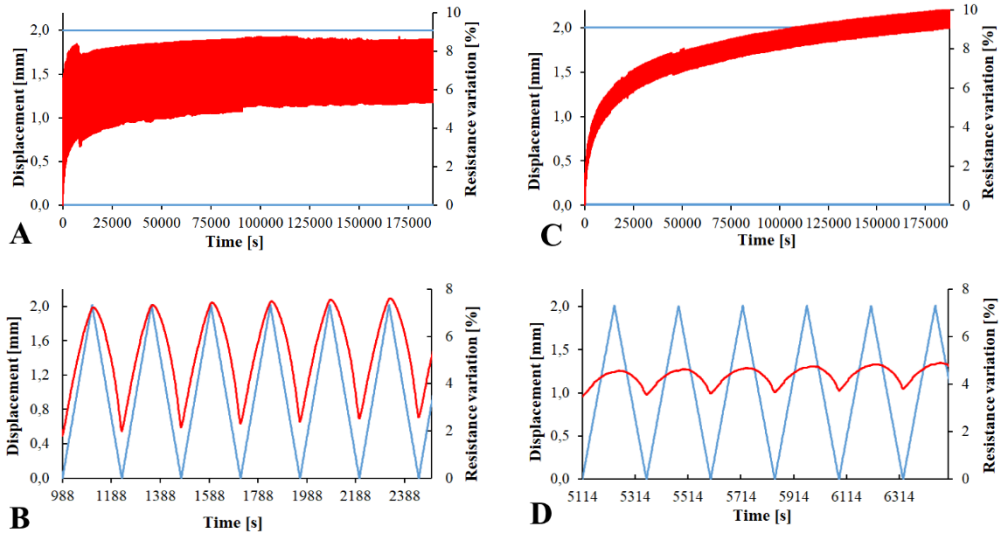

Figure 9

Tables

Table 1. Surface resistance of composites with different percent of CNTs

Sample	Resistance (kΩ/cm)
SEBS-3	3400 ± 1358
SEBS-4	86.5 ± 31.7
SEBS-5	3.25 ± 1.50
SEBS-6	0.37 ± 0.09
SEBS-7	0.12 ± 0.09

Table 2. Loading/unloading tests of nanocomposites: values of adopted testing parameters.

Diplacement, Holding time	CNTs (%)	ΔR_1 (%)	ΔR_2 (%)	R_b (%)	t (s)	v_1 (Ω/s)	v_2 (Ω/s)	v_3 (Ω/s)	v_3/v_2
2mm,2s	*5*	-0.32	-0.03	-0.73	(*)	-2.09	-2.60	-0.87	0.34
	6	0.14	-0.01	-0.15	0.28	0.17	-0.01	-0.13	18.85
2mm,5s	*5*	0.13	-0.04	-0.30	4.91	1.04	-0.81	-1.18	1.47
	6	0.03	-0.03	-0.17	7.80	0.067	-0.08	-0.07	0.90
2mm,10s	*5*	0.09	-0.09	-0.36	11.19	1.68	-1.92	-2.30	1.20
	6	0.07	-0.04	-0.17	4.30	0.08	-0.07	-0.78	10.68
5mm,2s	*5*	0.34	-0.02	-0.32	9.20	2.57	-2.10	-2.63	1.25
	6	0.36	-0.02	-0.18	1.50	0.17	-0.08	-0.16	2.04
5mm,5s	*5*	0.51	-0.03	-0.18	16.60	3.49	-1.31	-2.70	2.03
	6	0.67	-0.05	0.04	(*)	0.29	-0.10	-0.17	1.70
5mm,10s	*5*	0.42	-0.10	-0.31	10.76	1.30	-0.99	-1.30	1.31
	6	0.22	-0.11	-0.43	23.78	0.16	-0.28	-0.26	0.92
10mm,2s	*5*	0.98	-0.03	-0.24	36.40	2.30	-3.88	-2.24	0.58
	6	0.58	-0.02	-0.03	99.74	0.32	-0.27	-0.31	1.13
10mm,5s	*5*	1.45	-0.06	0.22	(*)	2.20	-0.92	-1.22	1.20
	6	0.92	-0.06	-0.01	115.40	0.34	-0.25	-0.22	0.89
10mm,10s	*5*	1.81	-0.08	0.46	(*)	6.80	-1.31	-5.22	3.98
	6	0.42	-0.12	-0.54	44.27	0.25	-0.35	-0.35	1.00

(*) The sample never recovered the pristine resistance value during the test.

724 **Table 3**. Set of parameters for the laser writing trials and resulting electrical resistance.

			SEBS-3			SEBS-4		
Trial	**V (mm/s)**	**P (%)**	**N repetition**	**R_t (kΩ/cm)**	**R_i (kΩ/cm)**	**N repetition**	**R_t (kΩ/cm)**	**R_i (kΩ/cm)**
T1	300	5	30	57.84 ± 35.22	OR	15	16.15 ± 0.18	OR
T2	200	5	30	12.32 ± 3.55	OR	15	13.85 ± 0.25	OR
T3	100	5	30	11.63 ± 3.11	34994 ± 1	15	5.85 ± 0.05	43700 ± 1
T4	300	10	30	2.23 ± 0.13	2980 ± 2	15	4.83 ± 0.54	440 ± 5
T5	200	10	30	1.55 ± 0.18	79 ± 1	15	0.47 ± 0.14	2.1 ± 0.1
T6	100	10	30	0.89 ± 0.1	11 ± 1	15	1.00 ± 0.07	6.7 ± 0.1
T7	300	20	30	0.57 ± 0.07	2.8 ± 0.2	15	1.11 ± 0.18	4.3 ± 0.3
T8	200	20	30	0.21 ± 0.04	0.8 ± 0.1	15	0.49 ± 0.08	1.9 ± 0.1
T9	100	20	30	/	/	15	0.24 ± 0.03	0.9 ± 0.1
T10	300	5	20	49.16 ± 35.84	OR	10	14.31 ± 1.01	OR
T11	200	5	20	21.44 ± 2.11	OR	10	10.01 ± 0.14	OR
T12	100	5	20	8.47 ± 4.20	25400 ± 1	10	3.77 ± 0.65	OR
T13	300	10	20	1.94 ± 0.31	14 ± 1	10	4.92 ± 0.10	9700 ± 99
T14	200	10	20	2.71 ± 0.06	3900 ± 11	10	2.03 ± 0.97	9.5 ± 0.6
T15	100	10	20	1.32 ± 0.11	54.5 ± 0.1	10	2.15 ± 0.30	11.2 ± 0.1
T16	300	20	20	2.00 ± 0.32	13.4 ± 0.1	10	6.11 ± 0.48	84 ± 1
T17	200	20	20	0.80 ± 0.19	3.4 ± 0.3	10	0.49 ± 0.08	1.8 ± 0.1
T18	100	20	20	/	/	10	0.18 ± 0.01	0.7 ± 0.1
T19	300	5	10	57.66 ± 9.11	OR	5	49.2 ± 16.30	OR
T20	200	5	10	47.73 ± 22.84	OR	5	57.56 ± 22.89	OR
T21	100	5	10	22.74 ± 0.40	OR	5	15.48 ± 1.28	OR
T22	300	10	10	10.64 ± 0.46	6.1 ± 0.1	5	19.5 ± 3.63	OR
T23	200	10	10	5.65 ± 1.01	120 ± 1	5	12.79 ± 2.69	3050 ± 3
T24	100	10	10	4.89 ± 0.26	250 ± 3	5	3.64 ± 1.96	17.4 ± 0.1
T25	300	20	10	8.86 ± 1.54	250 ± 2	5	14.51 ± 1.04	OR
T26	200	20	10	2.55 ± 0.17	11 ± 1	5	9.61 ± 0.51	OR
T27	100	20	10	0.66 ± 0.17	2.5 ± 1.0	5	0.97 ± 0.14	3.2 ± 0.1

725
726
727
728
729
730